Bar-Grid Oscillators

ZOYA BASTA POPOVIĆ, ROBERT M. WEIKLE II, MOONIL KIM, KENT A. POTTER, AND DAVID B. RUTLEDGE, SENIOR MEMBER, IEEE

Abstract — **Grid oscillators are an attractive way of obtaining high power levels from solid-state devices, since potentially the output powers of thousands of individual devices can be combined. The active devices do not require an external locking signal and the power combining is done in free space. In this work, 36 transistors are mounted on parallel brass bars, which provide a stable bias and have a low thermal resistance. The output power degrades gradually when devices fail. The grid gives an effective radiated power (*ERP*) of 3 W at 3 GHz. The directivity is 11.3 dB and the dc to RF efficiency is 22 percent. Modulation capabilities of the grid are demonstrated. An equivalent circuit model for the grid is derived, and comparison with experimental results is shown.**

I. Introduction

IN THE MICROWAVE and millimeter-wave region solid-state oscillators have limited output power levels. Compared to vacuum tubes, they are more compact, more reliable, less expensive, and require lower voltage power supplies. The output power available from individual solid-state oscillators is on the order of a watt at 10 GHz, falls to 100 mW at 100 GHz, and drops drastically at higher frequencies. It would be very useful to combine the output powers of a large number of solid-state devices. Classical power-combining schemes were developed in waveguide cavities [1], but they become impractical at millimeter-wave frequencies, since the waveguide dimensions become very small and losses in the metal walls high. Mink [2] suggested combining a large number of devices in a Fabry–Perot resonator. In this paper we demonstrate a quasi-optical approach where a grid loaded with transistors is placed inside a Fabry–Perot cavity (Fig. 1). This configuration is analogous to a laser, where the grid is the active medium. The grid presents an active surface with a reflection coefficient greater than unity for plane waves, which allows oscillations to build up. At the onset of oscillation different modes of the cavity compete, as in a laser. The mode with the lowest diffraction losses dominates, so that the output power is in one mode. The individual devices lock to this mode.

A wide variety of loaded grids have been demonstrated previously, including detectors [3], phase shifters [4], multipliers [5], and oscillators [6], [7]. These devices are suitable for large-scale monolithic integration. For example, the phase-shifting grid [4] had 1600 Schottky diodes monolithically fabricated in GaAs. The previous MESFET oscillator grid [6] was a hybrid circuit with 25 transistors. It was built on a quarter-dielectric-wavelength-thick grounded microstrip substrate and oscillated at 10 GHz. The source leads of the transistors went through the substrate and were soldered to the ground plane. The grid had an effective radiated power (*ERP*) of 37 W, a directivity of 16 dB, and a dc to RF efficiency of 15 percent.

In this paper we present a different design with 36 MESFET's mounted on a grid of metal bars. The bars provide excellent heat sinking and bias connections. Adjacent rows of the grid share gate and drain bias bars to minimize the number of bias voltages (Fig. 2). The grid is 0.6λ across, and the period is 10 mm ($\lambda/10$). The transistors used are Fujitsu low-noise MESFET's (FSC11LF) made for satellite receivers at 4 GHz. These devices typi-

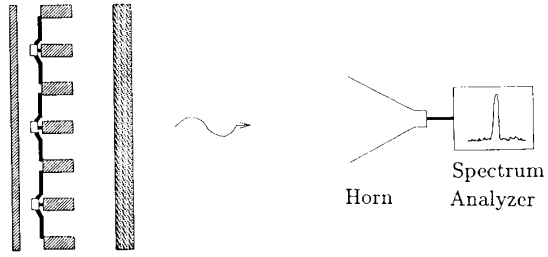

Fig. 1. Transistor bar-grid oscillator configuration.

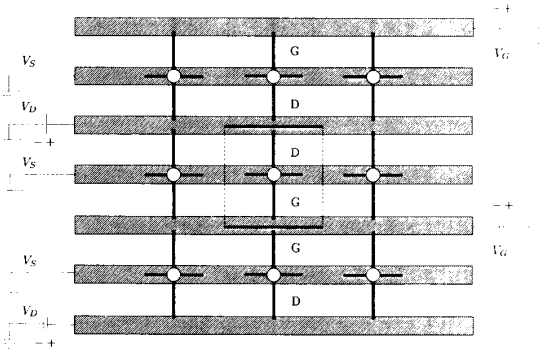

Fig. 2. Boundary conditions on the symmetry lines define the unit cell. The solid lines on top and bottom represent electric walls, and the dashed lines on the sides, magnetic walls. Adjacent rows share drain and gate biases.

Manuscript received August 10, 1989; revised November 6, 1989. This work was supported by the Army Research Office and the Northrop Corporation.

The authors are with the Division of Engineering and Applied Science, California Institute of Technology, Pasadena, CA 91125.

IEEE Log Number 8933248.

0018-9480/90/0300-0225$01.00 ©1990 IEEE

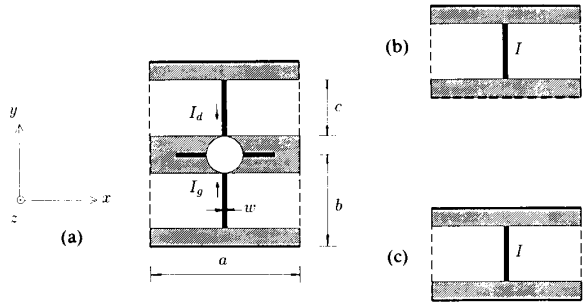

Fig. 3. The unit cell consists of two waveguides: one excited by the drain current and the other by the gate. Odd and even combinations of the currents reduce the unit cell (a) to (b) and (c), where the electric walls are represented with solid lines, and the magnetic walls with dashed ones.

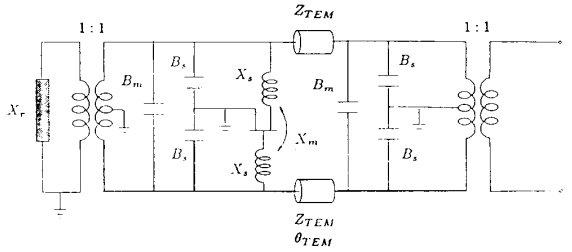

Fig. 4. Equivalent transmission-line circuit for transistors in the grid.

cally give an output power of 20 mW in single-transistor oscillators.

II. Transmission-Line Model for the Grid

The goal of the analysis is to find the reflection coefficient of an infinite grid for a plane wave at normal incidence. Strictly speaking, this analysis should be accurate only for grids that are much larger than a free-space wavelength. The symmetry of the grid imposes boundary conditions, which define a unit cell, shown in Fig. 2. This reduces the problem of analyzing the grid to that of analyzing an equivalent waveguide. The equivalent waveguide has electric walls (tangential electric field is zero) on the top and bottom, has magnetic walls (tangential magnetic field is zero) on the sides, and extends in the $+z$ and $-z$ directions, with the transistors in the $z = 0$ plane.

In order to model the behavior of the transistors in the grid, the impedances presented at the device terminals need to be found. The propagating mode has a real wave impedance and can be modeled with a TEM transmission line. The reactive impedances arise from the coupling between the currents in the leads and the evanescent modes. The method used to find these mode impedances is dual to the EMF analysis in the paper by Eisenhart and Kahn [8] for a post in a rectangular waveguide, and is similar to the analysis in [3]. Our problem is different, since there are two waveguides in the unit cell, as shown in Fig. 3. This introduces an additional mutual capacitance and inductance, which can be found by considering the odd and even combinations of the currents and voltages.

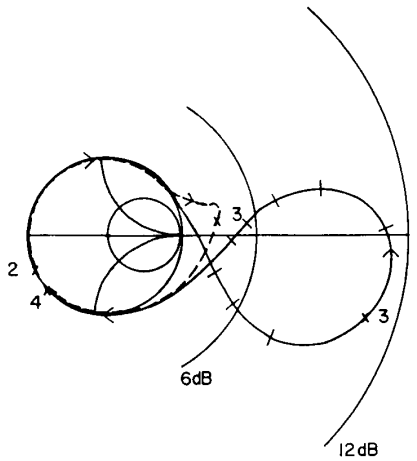

Fig. 5. Simulation of the transmission-line equivalent circuit. The dashed line shows the circuit behavior when the transistors are not saturated. The solid line shows the saturated behavior with a counterclockwise loop.

For example, when both the drain and the gate current are flowing into the transistor (Fig. 3(a)), the tangential magnetic fields cancel at the symmetry plane in the middle of the source bar, so we can place a magnetic wall (Fig. 3(b)). If one of the currents changes direction, an electric wall can be placed at the symmetry plane (Fig. 3(c)). The inductive self-reactance X_s of each lead is the average of the electric wall and magnetic wall reactances, and the mutual inductive reactance X_m is half the difference of the two. The currents and the fields are expanded in terms of the waveguide modes. Since the transistor leads are short compared to a wavelength, the currents are assumed to be uniform in the x and y directions. The self and mutual inductive reactances are given by

$$X_{s,m} = \frac{1}{2}\sum_{m=1}^{\infty} \operatorname{sinc}^2\left(\frac{m\pi w}{a}\right) \cdot \left(\frac{1}{\frac{a}{2}\left(\frac{1}{b}+\frac{1}{c}\right)Y_{m0} + \frac{a}{b}\sum\limits_{\substack{n=1\\ n\ \text{even}}}^{\infty} Y_{mn}\operatorname{sinc}^2\left(\frac{n\pi c}{2b}\right)} \pm \frac{1}{\frac{a}{2c}Y_{m0} + \frac{a}{b}\sum\limits_{\substack{n=1\\ n\ \text{odd}}}^{\infty} Y_{mn}\operatorname{sinc}^2\left(\frac{n\pi c}{4b}\right)} \right) \quad (1)$$

where the $+$ sign applies to the self and the $-$ sign to the mutual reactance; a, b, c, and w are the dimensions in the unit cell (Fig. 3); and Y_{mn} is the mnth mode admittance, given by

$$Y_{mn} = \omega\mu_0 \frac{\left(\frac{2m\pi}{a}\right)^2 - k^2}{\sqrt{\left(\frac{2m\pi}{a}\right)^2 - \left(\frac{n\pi}{b}\right)^2 - k^2}}. \quad (2)$$

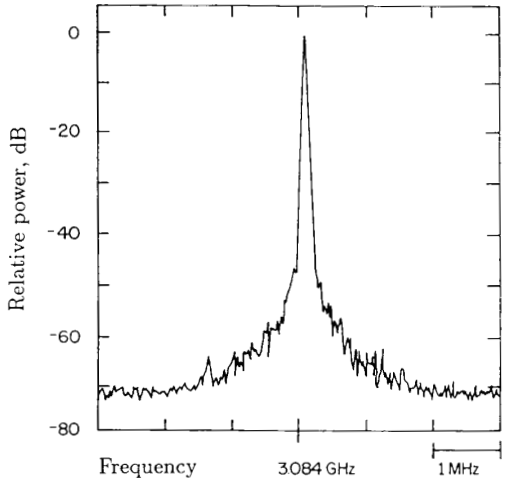

Fig. 6. Spectrum of a locked 36-MESFET grid oscillator.

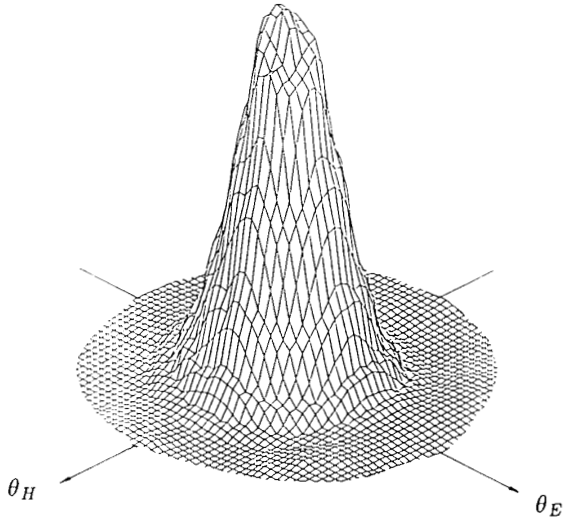

Fig. 7. Far-field radiation pattern of the grid oscillator. The axes are given in terms of spherical coordinates by $\theta_E = \theta \sin\phi$ and $\theta_H = \theta \cos\phi$. The vertical scale is linear in power.

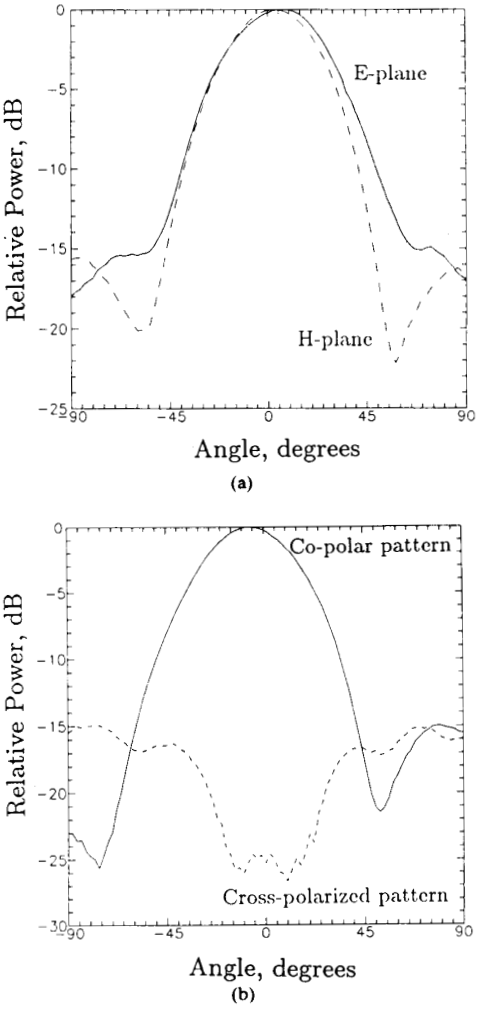

Fig. 8. (a) The *E*- and *H*-plane patterns of the grid-oscillator. (b) The 45° plane copolar and cross-polarized patterns.

In a similar fashion, the capacitive self and mutual susceptances are found. They are given by

$$B_s = \frac{a}{b} \sum_{\substack{n=1 \\ n \text{ odd}}}^{\infty} Y_{0n} \operatorname{sinc}^2\left(\frac{n\pi c}{4b}\right) \tag{3}$$

$$B_m = \frac{a}{b} \sum_{\substack{n=1 \\ n \text{ odd}}}^{\infty} Y_{0n} \operatorname{sinc}^2\left(\frac{n\pi c}{4b}\right) - \frac{a}{2b} \sum_{\substack{n=2 \\ n \text{ even}}} Y_{0n} \operatorname{sinc}^2\left(\frac{n\pi c}{2b}\right). \tag{4}$$

The equivalent circuit for the transistors in the grid is shown in Fig. 4. The center-tap transformer describes the coupling into free space, and the effect of the mirror is represented as a shunt reactance. The parameters at the 3 GHz operating frequency, with $a = 10$ mm, $b = 5$ mm, $c = 3$ mm, and $w = 0.75$ mm, are $Z_{\text{TEM}} = 188\ \Omega$, $\theta_{\text{TEM}} = 45°$, $X_s = 30\ \Omega$, $X_m = 0.25\ \Omega$, $B_x = 1.33$ mS, and $B_m = -0.57$ mS.

The simulation of the circuit was done with a microwave CAD program called *Puff*, developed at Caltech [9]. The simulation predicts an oscillation frequency of 3 GHz, which agrees with experiment. Fig. 5 shows the grid reflection coefficient on a Smith chart with a radius of 4 (12 dB). An instability is manifested as a counterclockwise loop on the Smith chart, and the oscillation frequency occurs where the magnitude of the reflection coefficient is the largest. To illustrate this behavior, also plotted on the same Smith chart is the reflection coefficient with the small-signal transistor *s* parameters. Saturation in oscillation is simulated by reducing the transistor s_{21} parameter by 3 dB, which shows the counterclockwise loop.

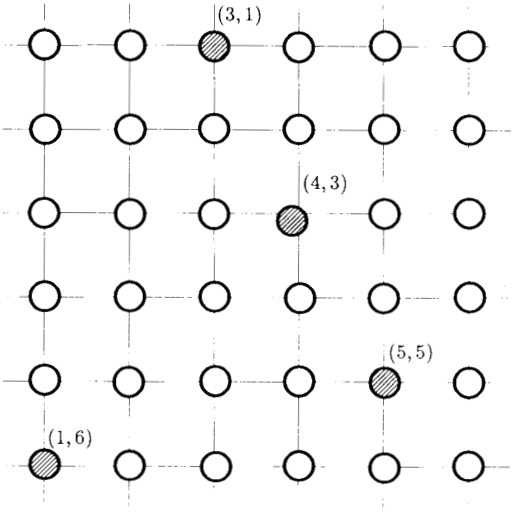

(a)

Removed devices	ΔP (dB)
(4,3)	−1.5
(5,5)	−2.0
(3,1)	−2.0
(1,6)	−2.0
(1,6), (3,1)	−6.0
(1,6), (3,1), (5,5)	−7.5
(1,6), (5,5), (3,1), (4,3)	−8.5

(b)

Fig. 9. (a) Grid schematic with removed devices indicated. (b) The degradation of power as devices were taken out of the grid. The first four rows are for devices removed one at a time, and in the last three they are taken out consecutively.

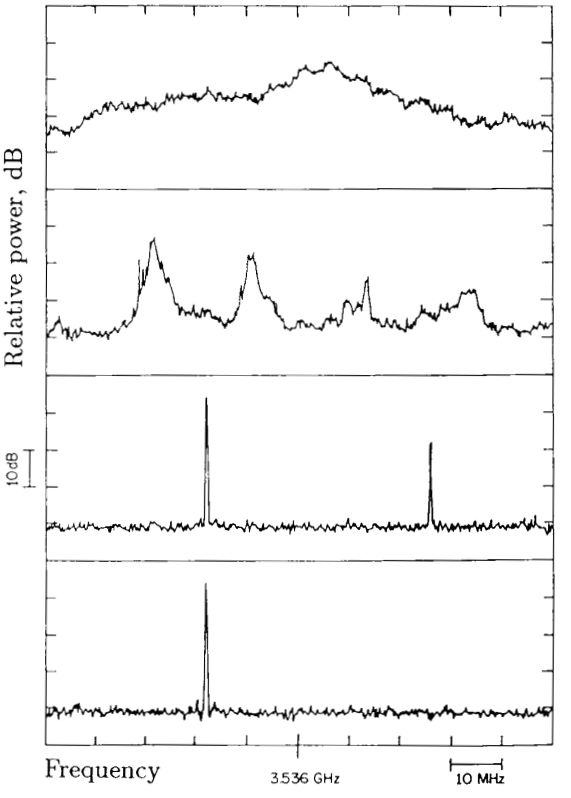

Fig. 10. Locking sequence of the oscillator. The successive spectra are recorded as the gate bias was varied. The unlocked grid spectrum is shown on the top figure. Locking starts in the next figure, where different bumps in the spectrum can be associated with different rows of the grid, and they narrow as the locking continues. These modes compete showing mixing products and locking finally occurs when they all lock to one of the modes. This sequence is similar to an injection-locking sequence, in which the different modes of the oscillator lock to one of the modes of the oscillator itself, rather than to an external locking signal.

III. Pattern Measurements

The locked spectrum of the grid is shown in Fig. 6. It is stable to within 2 MHz during 24 hours of CW operation. It is not sensitive to vibrations, and this was verified when the antenna pattern of the grid was measured by rotating it in a mount with stepper motors. The mirror is very close to the transistors—only 3 mm away. There were two dielectric slabs placed in front of the grid for impedance matching. The dielectric constant of the slabs is 12, they are 2 mm thick, and they are placed 20 and 35 mm in front of the grid. The measured far-field pattern of the grid is shown in Fig. 7. The directivity is calculated from the measured copolar pattern to be 11.3 dB. A power meter and a wide-band horn with a 9 dB gain were used to measure an *ERP* of 3.0 W. The input dc power is 1.0 W, and the calculated radiated power is 0.22 W. This gives a dc to RF efficiency of 22 percent, and an isotropic conversion gain of 4.8 dB. The isotropic conversion gain is a concept introduced by Stephan and Itoh [10] and is the product of the efficiency and the directivity. Fig. 8 shows the *E*- and *H*-plane patterns (a) and the copolar and cross-polarized patterns (b) in the 45° plane. In this mode of operation the frequency of the grid can be tuned over 300 MHz by moving the mirror.

The effect of device failures was tested by removing devices indicated in Fig. 9(a). Fig. 9(b) shows the received power after removing devices labeled according to their position in the grid.

The grid has an interesting locking sequence, which is illustrated in Fig. 10. These spectra were recorded as the gate bias was varied over a range of 1 V. Qualitative probing shows that first the devices in individual rows lock, and then adjacent rows lock together. A similar behavior is observed when the mirror position is varied.

IV. Modulation Measurements

Another mode of operation at a lower drain current and larger mirror spacing gives lower power, but allows electrical modulation through the bias lines. The gate voltage modulates the frequency over 300 MHz (250 MHz/V). The drain voltage has more effect on the amplitude, so

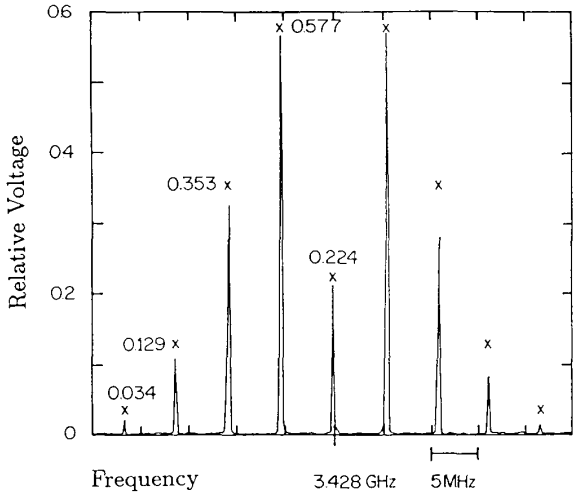

Fig. 11. Measured grid oscillator FM spectrum. The scale is linear in voltage and the numbers at the ×'s give Bessel-function coefficients.

there is a possibility for AM or FM. Fig. 11 shows a measured FM spectrum, with a modulation frequency of 5 MHz and a modulation index β of 2. The FM spectrum is given by [11]

$$x(t) = A \sum_{n=-\infty}^{\infty} J_n(\beta) \cos 2\pi (f + nf_m)t. \qquad (5)$$

The calculated Bessel coefficients are indicated in Fig. 11, and they agree well with the experiment.

V. Conclusion

The grid oscillator presented in this paper is both an antenna and a source. In an antenna application, the important parameters would be the effective radiated power (*ERP*), isotropic conversion gain, and antenna pattern. In a source application the grid might be used as a feed for a lens or a reflector, in which case the radiated power and the efficiency are of interest. The grid is attractive because of its simplicity. It should be possible to make a monolithic grid mounted on bars for heat removal. It is suitable for millimeter-wave applications. At smaller wavelengths a grid of the same size would be many wavelengths across, and this would make the beam narrower and increase the effective radiated power.

References

[1] K. Kurokawa, "The single-cavity multiple-device oscillator," *IEEE Trans. Microwave Theory Tech.*, vol. MTT-19, pp. 793–801, Oct. 1971.

[2] J. W. Mink, "Quasi-optical power combining of solid-state millimeter-wave sources," *IEEE Trans. Microwave Theory Tech.*, vol. MTT-34, pp. 273–279, Feb. 1986.

[3] D. B. Rutledge and S. E. Schwarz, "Planar multimode detector arrays for infrared and millimeter-wave applications," *IEEE. Quantum Electron.*, vol. QE-17, pp. 407–414, Mar. 1981.

[4] W. W. Lam *et al.* "Millimeter-wave diode-grid phase shifters," *IEEE Trans. Microwave Theory Tech.*, vol. 36, pp. 902–907, May 1988.

[5] C. F. Jou *et al.* "Millimeter-wave diode-grid frequency doubler," *IEEE Trans. Microwave Theory Tech.*, vol. 36, pp. 1507–1514, Nov. 1988.

[6] Z. B. Popovic, M. Kim, and D. B. Rutledge, "Grid oscillators," *Int. J. Infrared and Millimeter Waves*, vol. 9, no. 7, pp. 647–654, July 1988.

[7] M. Hieda, M. Nakayama, K. Mizuno, T. Ajikata, and D.Rutledge, "Quasi-optical resonator for millimeter and submillimeter wave solid-state sources," in *Proc. 13th Int. Conf. Infrared and Millimeter Waves*, Dec. 1988, pp. 55–56.

[8] R. L. Eisenhart and P. J. Kahn, "Theoretical and experimental analysis of a waveguide mounting structure," *IEEE Trans. Microwave Theory Tech.* vol. MTT-19, pp. 706–719, Aug. 1971.

[9] R. C. Compton and D. B. Rutledge, "*Puff*—Computer Aided Design for Microwave Integrated Circuits," program manual, pp. 26, 1987. Available from the authors.

[10] C. Stephan and T. Itoh, "Planar quasi-optical subharmonically pumped mixer characterized by isotropic conversion loss," *IEEE Trans. Microwave Theory Tech.*, vol. MTT-32, pp. 97–102, Jan. 1984.

[11] R. E. Ziemer and W. H. Tranter, *Principles of Communications*. Boston: Houghton Mifflin, 1976, pp. 117.

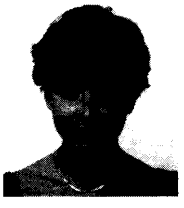

Zoya Basta Popović was born in Belgrade, Yugoslavia, on May 10, 1962. She graduated with the Dipl. Ing. (B.Sc.) degree from the Electrical Engineering Department of the University of Belgrade in 1985. In 1986 she obtained the M.S. degree from the California Institute of Technology, where she is now doing research toward the Ph.D. in the Millimeter-Wave Integrated Circuit group. Her main areas of interest are quasi-optical microwave and millimeter-wave power-combining and millimeter-wave printed circuit antennas.

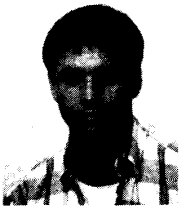

Robert M. Weikle II was born in Tacoma, WA, on February 13, 1963. He received the B.S. degree in electrical engineering and physics from Rice University, Houston, TX, in 1986 and the M.S. degree in electrical engineering from Caltech in 1987. His research interests include high-frequency solid-state devices and millimeter-wave quasi-optical techniques. Currently, he is working toward the Ph.D. degree at Caltech.

Mr. Weikle is a member of Phi Beta Kappa, Tau Beta Pi, and the American Physical Society.

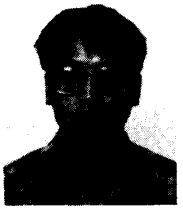

Moonil Kim was born in Seoul, Korea, on March 14, 1965. He received the B.S. degree from the Illinois Institute of Technology in 1987 and the M.S. degree from the California Institute of Technology in 1988. He is currently working toward the Ph.D. in the MMIC group at the California Institute of Technology. He has been working on millimeter-wave power combining and beam steering circuitry.

Kent A. Potter received the B.S. degree in physics from California State University, Long Beach, in 1976.

From 1976 to 1986 he was associated with the GALCIT Ten Foot Wind Tunnel in the Department of Aeronautics at Caltech, working with instrumentation and data acquisition systems. Since 1986 he has served as laboratory engineer in the Electrical Engineering and Applied Physics Departments at Caltech, supporting work in millimeter and microwaves, with emphasis on instrumentation and electromechanical design.

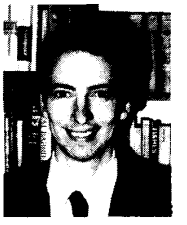

David B. Rutledge (S'77– M'80–SM'89) was born in Savannah, GA, on January 12, 1952. He received the B.A. degree in mathematics from Williams College, Williamstown, MA, in 1973, the M.A. degree in electrical sciences from Cambridge University, Cambridge, England, in 1975, and the Ph.D. degree in electrical engineering from the University of California at Berkeley in 1980.

In 1980 he joined the faculty at the California Institute of Technology, Pasadena, CA, where he is now Professor of Electrical Engineering. His research is in developing millimeter- and submillimeter-wave monolithic integrated circuits and applications, and in software for computer-aided design and measurement. He is coauthor, with Prof. R. Compton of Cornell University, of the software CAD program *Puff*, which has over 6000 users worldwide.